component with $T_d = 50$ K that produces the far-infrared. The far-infrared luminosity, 22% of the total, may correspond to the luminosity generated by star formation deduced above. The ratio $L_{FIR}/L'_{HCN} = 1{,}700$ is then comparable to that of ultraluminous IR galaxies.

Adopting the Arp220 comparison for the expected ratio L_{FIR}/L'_{HCN} yields a star formation rate of 10^3 solar masses per year for the Cloverleaf, 300 times the rate in the Milky Way and 30 times greater than that of optical–ultraviolet starburst galaxies. The dense gas depletion time or starburst lifetime is about 10^7 years. Thus, in addition to the quasar, the Cloverleaf galaxy appears to have a huge starburst, more luminous than any optical starburst and comparable to that in ultraluminous IR galaxies. □

Received 9 June; accepted 10 October 2003; doi:10.1038/nature02149.

1. Penzias, A. A., Solomon, P. M., Wilson, R. W. & Jefferts, K. B. Interstellar carbon monosulfide. *Astrophys. J.* **168,** L53–L58 (1971).
2. Solomon, P. M., Jefferts, K. B., Penzias, A. A. & Wilson, R. W. Interstellar methyl cyanide. *Astrophys. J.* **168,** L107–L110 (1971).
3. Plume, R., Jaffe, D. T., Evans, N. J. II, Martin-Pintado, J. & Gomez-Gonzalez, J. Dense gas and star formation: Characteristics of cloud cores associated with water masers. *Astrophys. J.* **476,** 730–749 (1997).
4. Solomon, P. M., Downes, D. & Radford, S. J. E. Dense molecular gas and starbursts in ultra-luminous galaxies. *Astrophys. J.* **387,** L55–L59 (1992).
5. Barvainis, R., Tacconi, L., Antonucci, R., Alloin, D. & Coleman, P. Extremely strong carbon-monoxide emission from the Cloverleaf quasar at a redshift of 2.5. *Nature* **371,** 586–588 (1994).
6. Barvainis, R., Maloney, P., Antonucci, R. & Alloin, D. Multiple CO transitions, C I, and HCN from the Cloverleaf quasar. *Astrophys. J.* **484,** 695–701 (1997).
7. Weiss, A., Henkel, C., Downes, D. & Walter, F. Atomic carbon in the Cloverleaf quasar at redshift of 2.5. *Astron. Astrophys.* (submitted).
8. Venturini, S. & Solomon, P. M. The molecular disk in the Cloverleaf quasar. *Astrophys. J.* **590,** 740–745 (2003).
9. Gao, Y. & Solomon, P. M. Star formation rate and dense molecular gas in galaxies. *Astrophys. J.* (submitted). Preprint at ⟨http://arXiv.org/astro-ph/0310339⟩ (2003).
10. Kneib, J.-P. *et al.* Modelling the Cloverleaf: Contribution of a galaxy cluster at z ~ 1.7. *Astron. Astrophys.* **329,** 827–839 (1998).
11. Solomon, P. M., Downes, D., Radford, S. J. E. & Barrett, J. W. The molecular interstellar medium in ultra-luminous infrared galaxies. *Astrophys. J.* **478,** 144–161 (1997).
12. Downes, D. & Solomon, P. M. Rotating nuclear rings and extreme starbursts in ultra-luminous galaxies. *Astrophys. J.* **507,** 615–654 (1998).
13. Granato, G. L., Danese, L. & Franceschini, A. Dust-enshrouded AGN models for hyperluminous, high-redshift infrared galaxies. *Astrophys. J.* **460,** L11–L14 (1996).
14. Carilli, C. *et al.* A molecular Einstein ring: Imaging a starburst disk surrounding a quasi-stellar object. *Science* **300,** 773–775 (2003).

Acknowledgements We thank D. Downes for discussions. The National Radio Astronomy Observatory is operated by Associated Universities, Inc., under cooperative agreement with the National Science Foundation. P.V.B. thanks Columbia University and the Institut d'Astrophysique de Paris for hospitality during this research.

Competing interests statement The authors declare that they have no competing financial interests.

Correspondence and requests for materials should be addressed to P.M.S. (psolomon@sbastk.ess.sunysb.edu).

Stationary pulses of light in an atomic medium

M. Bajcsy[1,2], A. S. Zibrov[1,3,4] & M. D. Lukin[1]

[1]*Physics Department,* [2]*Division of Engineering and Applied Sciences, Harvard University,* [3]*Harvard-Smithsonian Center for Astrophysics, Cambridge, Massachusetts 02138, USA*
[4]*Lebedev Institute of Physics, Moscow, 117924 Russia*

Physical processes that could facilitate coherent control of light propagation are under active exploration[1–5]. In addition to their fundamental interest, these efforts are stimulated by practical possibilities, such as the development of a quantum memory for photonic states[6–8]. Controlled localization and storage of photonic pulses may also allow novel approaches to manipulating of light via enhanced nonlinear optical processes[9]. Recently, electromagnetically induced transparency[10] was used to reduce the group velocity of propagating light pulses[11,12] and to reversibly map propagating light pulses into stationary spin excitations in atomic media[13–16]. Here we describe and experimentally demonstrate a technique in which light propagating in a medium of Rb atoms is converted into an excitation with localized, stationary electromagnetic energy, which can be held and released after a controllable interval. Our method creates pulses of light with stationary envelopes bound to an atomic spin coherence, offering new possibilities for photon state manipulation and nonlinear optical processes at low light levels.

Several techniques to generate stationary light pulses in an atomic medium have recently been proposed theoretically[17,18]. The present work is related conceptually to the ideas of ref. 18, but here we use a different approach that involves spatial modulation of the absorptive properties of the medium. The use of such a dissipative effect for coherent control of light is a novel phenomenon, closely related to earlier work on matched pulse propagation in electromagnetically induced transparency (EIT)[2,19]. Although there exists a substantial body of work on localization of light in random dielectrics[20], Bragg gratings and photonic bandgap materials[21–23], the unique feature of the present method is that it allows accurate control of the creation of a stationary light pulse and its release.

The present method can be understood qualitatively by considering a three-state 'lambda' configuration of atomic states (Fig. 1a). A large ensemble of N atoms is initially prepared in the ground state, $|g\rangle$. We use forward and backward control beams, with time varying Rabi frequencies $\Omega_+(t)$ and $\Omega_-(t)$, respectively, to manipulate a weak pulse of signal light. In our experimental realization, the two control fields have identical frequencies but opposite propagation directions. The usual EIT[10] corresponds to simultaneous propagation of the forward control and signal beams. When their frequency difference matches the level splitting between the ground state and a metastable ('spin-flipped') state ($|s\rangle$) the medium becomes transparent for the signal light, while the sharp atomic dispersion allows one to slow and localize an input signal pulse in the medium[11,12]. By turning the control beam off while the pulse is in the medium[13], the signal amplitude vanishes while its state is stored in a stationary spin coherence. This atomic excitation can be converted back into a light pulse, propagating in the forward or the backward direction, by application of the corresponding control beam[14–16]. The atomic coherence can be converted into a stationary photonic excitation if the medium is illuminated simultaneously by forward and backward control beams. Specifically, if the two create a standing wave pattern, the EIT suppresses the signal absorption everywhere but in the nodes of the standing wave, resulting in a sharply peaked, periodic modulation of the atomic absorption for the signal light (Fig. 1b). Illumination by these beams also results in partial conversion of the stored atomic spin excitation into sinusoidally modulated signal light, but the latter cannot propagate in the medium owing to Bragg reflections off the sharp absorption peaks, resulting in vanishing group velocity of the signal pulse. Only after one of the control beams is turned off does the pulse acquire a finite velocity and can thus leave the medium in the direction of the remaining control beam.

To quantify these effects theoretically, we consider the interaction of atoms with resonant optical fields, represented by plane waves. We decompose the signal field into components propagating in the forward and backward directions along the z axis with wavevectors $\pm k$ and slowly varying amplitudes $E_\pm$. Following refs 13 and 18, we introduce two components $\Psi_\pm$ of a coupled excitation of light and an atomic spin wave ('dark-state polariton') corresponding to forward and backward signal fields, respectively. In the experimentally relevant case of small group velocities, the polariton components are represented by $\Psi_\pm = g\sqrt{N}E_\pm/\Omega_\pm$, where g is the atom–

field coupling constant[1]. Assuming further slowly varying pulses and negligible spin decoherence, we find that the components evolve according to:

$$\frac{\partial}{\partial z}\Psi_+ = -\alpha_-\xi(\Psi_+ - \Psi_-) - \frac{1}{c}\frac{\partial}{\partial\tau}(\alpha_+\Psi_+ + \alpha_-\Psi_-) \qquad (1)$$

$$\frac{\partial}{\partial z}\Psi_- = -\alpha_+\xi(\Psi_+ - \Psi_-) + \frac{1}{c}\frac{\partial}{\partial\tau}(\alpha_+\Psi_+ + \alpha_-\Psi_-) \qquad (2)$$

and the spin coherence $S = N^{-1/2}(\alpha_+\Psi_+ + \alpha_-\Psi_-)$ with $\alpha_\pm = |\Omega_\pm|^2/(|\Omega_+|^2 + |\Omega_-|^2)$. These equations describe two slow waves that are coupled owing to periodic modulation of atomic absorption and group velocity. The first term in the right-hand side of equations (1) and (2) is proportional to an absorption coefficient ξ near the resonant line centre (away from line centre ξ is imaginary and proportional to the dispersive phase shift of signal light). When ξ is large, this term gives rise to the pulse matching phenomenon[2,19]: whenever one of the fields is created, the other will adjust itself within a short propagation distance to match its amplitude such that $\Psi_+ - \Psi_- \to 0$. The scaled time, $\tau(t) = \int_0^t dt(|\Omega_+|^2 + |\Omega_-|^2)/g^2N$, reflects the group velocity reduction associated with atomic dispersion. Finally, the centre frequency of the signal light was chosen to match its wavevector to that of the periodic absorption modulation. Owing to the steep atomic dispersion, this condition can be satisfied by a small detuning of the signal light, in direct analogy with other EIT-based processes[2].

In the case when the forward signal field propagates in the presence of only one (forward) control field, equation (1) has a simple solution $\Psi_+(z,t) = \Psi_+(z - c\tau(t), 0)$, which describes a coherent deceleration (Fig. 1c). Specifically, when the forward control beam is turned off, the polariton is stopped, the signal light vanishes, and a stationary spin excitation is created. Note that the spatial length of the spin excitation, l, is determined by the length of the compressed pulse corresponding to a product of the input pulse duration and the initial group velocity v_g^0. Finally, when the forward control beam is turned back on, the propagating signal pulse is recreated.

When both control beams are turned on simultaneously, forward and backward signal components are both generated. The electric field amplitudes for both forward and backward signal light are proportional to the amplitudes of the corresponding control fields, as required by the pulse matching condition[2,19]. Interesting insight into the propagation dynamics can be gained by considering the dispersion relation associated with equations (1) and (2), $\omega =$

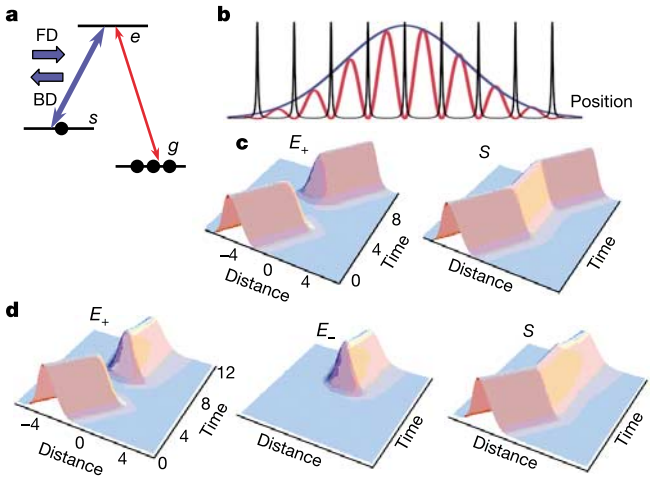

Figure 1 Physics of stationary pulses of light. **a**, Schematic of the atomic system. The signal beam (red arrow) is resonant with the transition from the ground to the excited state ($|e\rangle$) and the control fields (blue arrows: FD, forward; BD, backward) are tuned to resonance between the $|s\rangle$ state and the excited state. **b**, Schematic illustration of the spatial variation of the signal field absorption (black line), and the electric field (red line) in the stationary pulse in the medium along the direction of the control beam. Blue line represents initial atomic spin coherence. **c**, Storage of the weak signal pulse in Raman coherence. Calculated evolution is shown for the forward signal pulse and atomic spin wave amplitudes as a function of distance (in the units of compressed pulse length, l) and time (in units of l/v_g^0). While the forward pulse propagates the forward control beam is turned off (at the time $t = 4l/v_g^0$) and the pulse is stored in a stationary spin coherence. At the time $t = 8l/v_g^0$ the forward control field is turned back on, recreating the propagating pulse. Calculations are based on equations (1) and (2) with gaussian pulses and $\alpha_+ = 1, \alpha_- = 0$. **d**, Calculated evolution of the forward and backward signal components and atomic spin wave amplitude for the case when the stored coherence is illuminated (at time $t = 8l/v_g^0$) by forward and backward control beams with equal Rabi frequencies. Here stationary signal pulses are created. The main contributions to the dynamics include a slow spreading of the amplitudes as well as small shifts (of the order of $1/\xi$) of forward and backward components in the corresponding directions relative to the atomic coherence. Calculations are based on equations (1) and (2) with $\alpha_+ = \alpha_- = 1/2, \xi l = 10$. All simulations assume that $v_g \ll c$, in which case the polaritons are mostly atomic and the amplitude of the spin coherence does not change significantly while the pulse is in the medium. Amplitude of fields and coherence are normalized to their initial value at $t = 0$.

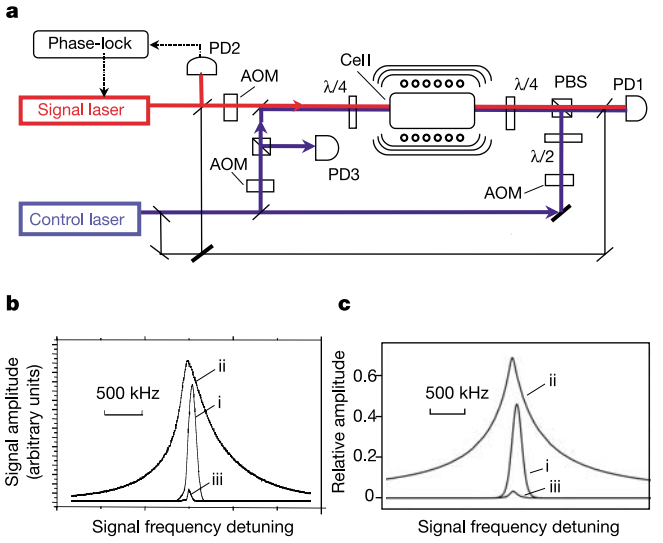

Figure 2 Experimental set-up, results of c.w. experiments and simulations. **a**, The signal field is generated by an extended cavity diode laser. The control beam from a locked Ti:sapphire laser is split to provide both forward and backward control fields. The signal laser is phase-locked to the control laser with a frequency offset corresponding to the hyperfine splitting of ^{87}Rb (6.84 GHz). All three fields have circular polarizations in the cell, but their intensities are controlled independently by acousto-optic modulators (AOMs). The beams overlap inside the cell at an angle of $\sim 10^{-4}$ rad. PD1 and PD3 are fast photodiodes used for heterodyne detection of the signal amplitude using a reference beam (black line). These are followed by a spectrum analyser running in zero span mode (the detection bandwidth is 3 MHz). The c.w. power of the signal beam is 250 μW, while the powers of the forward and backward control beams are independently adjusted between 8.0 mW and 40 mW. The beam size inside the cell is about 2 mm. $\lambda/2$ and $\lambda/4$ are half- and quarter-wave plates respectively. PBS, polarizing beam-splitter. **b**, Curve i represents the EIT signal transmission when the forward control beam is on and the backward control beam is off. Transmission is approximately 50% at EIT resonance. Curve ii is the reflected signal, and curve iii is the signal transmission when both forward and backward control fields are on. **c**, Corresponding theoretical simulations of the transmission and reflection of signal field from the medium composed of atoms as in Fig. 1a. Parameters correspond to atomic Rb, $\Omega_+ = \Omega_- = 15$ MHz, the spin decoherence rate of 3 kHz, and medium length corresponding to resonant attenuation of e^{-15}. The small frequency shift in the reflection resonance accounts for wavevector matching to satisfy the Bragg condition.

$-ck(\xi[\alpha_+ - \alpha_-] - ik)/(\xi - ik[\alpha_+ - \alpha_-])$, where ω is the Fourier frequency corresponding to the scaled time τ, and k is the spatial wavevector of the signal pulse envelopes. For small wavevectors and a large absorption coefficient, this corresponds to a linear dispersive medium with a group velocity $v_g = c(|\Omega_+|^2 - |\Omega_-|^2)/g^2N$. Thus, the time-domain solution describes the coupled motion of the $\Psi_\pm$ envelopes at a group velocity proportional to the intensity difference between the two control fields. When the control Rabi frequencies are identical, the group velocity v_g vanishes and a stationary pulse of light is created (Fig. 1d). The electric field amplitudes of two signal components are then equal, $E_+ = E_-$, corresponding to sinusoidally modulated signal intensity, and the dispersion relation becomes $\omega = ick^2/\xi$. In the time domain, this corresponds to a slow spreading of the stationary pulse at a rate $\delta l/l \approx c\tau/(\xi l^2)$, which determines the maximal holding time. Hence, in an optically dense medium ($\xi l \gg 1$) a stationary photonic excitation can be controllably created.

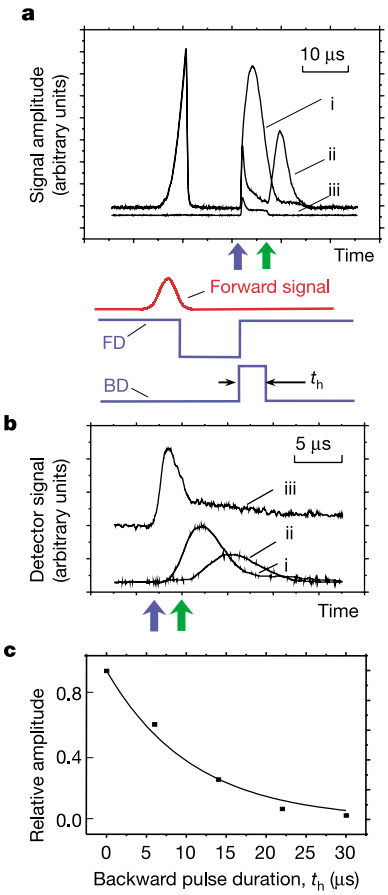

Figure 3 Results of pulsed experiments. **a**, Top, detected output signals from the Rb cell; bottom, timing diagram. Curve i is the signal detected in the forward direction resulting from pulse storage in a spin coherence. The left peak represents the fraction of the signal pulse that leaves the cell before the trapping has begun. (We were able to suppress this fraction to ~10%.) It is delayed by ~10 μs compared to the original pulse (see timing diagram). The right peak in curve i appears only after the forward control is turned on, and thus represents the stored and retrieved signal. Curve ii is the same except the forward and backward control beams (FD and BD) are both turned on, as shown on the timing diagram and marked by the blue arrow. Curve iii is the signal in the backward direction under the same conditions. (This curve is plotted on a different scale, with the peak signal about a factor of five weaker than that on curve ii). The pulse is released in the forward direction when the backward control is turned off (green arrow). On the timing diagram, the rise time edges of the control pulses are about 0.1 μs. Note that the frequencies of the two control fields do not need to be exactly equal. This is in agreement with theory, and was verified by obtaining results similar to those in curve ii with backward control beam shifted by 80 MHz from the forward control. **b**, Rb fluorescence measured at the side of the cell. Curve iii is fluorescence associated with signal light during the release with both forward and backward control beams on. Background fluorescence associated with control beams is subtracted. Curves i and ii (shown for reference) correspond to the same signals as curves i and ii in **a**. Note that fluorescence measurements are carried out under conditions differing from those for other data (including **a**), because the photodetector inserted inside the magnetic shields introduces stray magnetic fields resulting in shortened spin coherence and storage times; this measurement is also detection-bandwidth limited. **c**, Dependence of the released signal pulse magnitude on the backward control pulse duration t_h.

Our experimental apparatus used to demonstrate this effect is shown in Fig. 2a. A magnetically shielded 4-cm-long cell containing ^{87}Rb vapour is maintained at temperature $T \approx 90\,^{\circ}$C (atom number density is $10^{12} - 10^{13}\,\mathrm{cm}^{-3}$). Long-lived hyperfine sublevels of the electronic ground state $S_{1/2}$ with $F = 1,2$ are used as the storage states $|g\rangle$, $|s\rangle$, respectively, coupled via the excited state $P_{1/2}$. The hyperfine coherence time is limited by atomic diffusion out of the beam volume, and is enhanced with a Ne buffer gas at a pressure of 6 torr (resulting in spin-coherence lifetimes in the microsecond to millisecond range[12,15]). Note that the Doppler shifts due to atomic motion do not directly affect the spin coherence when the control and the signal beams propagate collinearly in forward and backward pairs.

We first consider continuous wave (c.w.) excitation of the atomic Rb. Without the control beams, the atomic medium is completely opaque to the forward signal beam. When the forward control field is present, a sharp resonance, a few hundred kilohertz wide, appears in the transmission spectrum of the signal beam, corresponding to EIT (curve i in Fig. 2b). Turning on the backward control beam in the c.w. regime greatly reduces the EIT transmission (curve iii), while at the same time generating a reflected signal beam that is detected in the backward direction (curve ii). The peak reflection intensity is a substantial fraction (up to ~80%) of the input signal beam.

These results demonstrate the possibility of coherent control of light via simultaneous driving of the medium with FD and BD control beams. Specifically, the signal light cannot propagate in the modulated EIT medium, but instead of absorbing the signal the medium reflects it as a high-quality Bragg mirror. This effect is analogous to that predicted theoretically[18]. However, the broad lineshape of curve ii indicates that periodic modulation (grating) of the absorptive rather than dispersive properties lies at the origin of the observed Bragg reflection[21]. We note, in particular, good agreement between the present experimental results and a theoretical model based on the resonant EIT medium with forward and backward control fields (Fig. 2c). At the same time, a qualitatively different lineshape is expected for dispersive Bragg gratings[18,23].

Turning to experiments with pulsed light, we first map the input signal pulse onto an atomic coherence of the Rb atoms[14,15]. This procedure corresponds to Fig. 1c, and its experimental observation is shown by curve i in Fig. 3a. The atoms are first optically pumped into the lowest state. A gaussian-shaped signal pulse of about 5 μs duration then enters the medium, where it is slowed to $v_g^0 \approx 6\,\mathrm{km\,s}^{-1}$. The forward control beam is subsequently turned off. As a rule, a fraction of the signal pulse leaves the cell before that, leading to the first peak of curve i. When the forward control field is turned back on, the stored atomic excitation is converted back into light, which is detected in the forward direction (second peak of curve i). The amplitude of the retrieved light decays with increasing storage interval with a characteristic timescale of about 20 μs, corresponding to decay of the hyperfine coherence caused by atomic diffusion. Similar experimental results are obtained by detecting the signal light in the backward direction when the stored coherence is retrieved with the backward control beam[16].

We next consider the retrieval of the atomic excitations by simultaneous application of the forward and backward control beams. When the intensities of the beams are carefully adjusted, the output signal pulses in both forward and backward directions

are greatly suppressed (curves ii and iii in Fig. 3a). Both channels exhibit small leakage. We attribute the first peak to photons retrieved near the cell boundaries, which do not experience sufficient Bragg reflections to be trapped efficiently. The long tail is probably due to a slow spreading of the stored pulse. When the backward beam is turned off, the released pulse is detected in the forward channel (curve ii). The presence of signal light inside the cell during the simultaneous application of the two control beams was verified directly by monitoring fluorescence from the side of the cell (Fig. 3b). For times when the signal output in the forward and backward directions is greatly suppressed, we observed significant enhancement of the signal light fluorescence (curve iii in Fig. 3b), due to residual atomic absorption.

These observations provide evidence for controlled conversion of the stored atomic coherence into a stationary photonic excitation in the cell. Note, in particular, that the magnitude of the fluorescence drops sharply after the backward pulse is turned off. This drop is followed by a gradual decay, associated with the exit of the slow pulse from the medium. This behaviour is in qualitative agreement with our simple model, which predicts the light intensity in the stationary pulses to be double that in the slowly propagating pulse. As shown in Fig. 3c, the magnitude of the released pulse decreases exponentially with increasing trapping time with a characteristic time constant of about 7 μs. Note that only a part of this decay is due to the hyperfine coherence decay. Other decay mechanisms include spreading of the stationary pulse, as well as imperfect EIT. We anticipate that improvements in efficiency can probably be achieved by initial optical pumping into a single atomic sublevel, using an atomic system with larger level spacing or using the sharper absorption lines of cold atom clouds.

We finally outline possible avenues opened by the present work. First, we note that our procedure is based on a passive medium, and in the ideal limit is not accompanied by optical loss or gain, hence avoiding the associated noise. We therefore anticipate that our method preserves the quantum states of light pulses. (This is in contrast to Bragg gratings based on gain modulation[21].) Second, although the present work demonstrates stationary light localization and storage in one dimension, it should be possible to controllably localize and guide stationary photonic pulses in three spatial dimensions by using control beams with properly designed wavefronts. Third, controlled conversion of propagating light into stationary light pulses opens interesting possibilities for enhanced nonlinear optical processes by combining the present technique with the resonant enhancement of nonlinear optics via EIT[24–26]. This combination may enable controlled interactions involving quantum few-photon fields[27–30] analogous to those feasible in cavity quantum electrodynamics[5]. Finally, extension of the present ideas to other systems might be possible using, for example, dynamic modulation of photonic bandgap materials. □

Received 6 September; accepted 4 November 2003; doi:10.1038/nature02176.

1. Scully, M. O. & Zubairy, S. M. *Quantum Optics* (Cambridge Univ. Press, Cambridge, UK, 1997).
2. Harris, S. E. Electromagnetically induced transparency. *Phys. Today* **50**(7), 36–42 (1997).
3. Lukin, M. D. & Imamoglu, A. Controlling photons using electromagnetically induced transparency. *Nature* **413,** 273–276 (2001).
4. Matsko, A. B. *et al.* Slow, ultraslow, stored, and frozen light. *Adv. At. Mol. Opt. Phys.* **46,** 191–242 (2001).
5. Mabuchi, H. & Doherty, A. C. Cavity quantum electrodynamics: Coherence in context. *Science* **298,** 1372–1377 (2002).
6. Cirac, J. I. *et al.* Quantum state transfer and entaglement distribution among distant nodes in a quantum network. *Phys. Rev. Lett.* **78,** 3221–3224 (1997).
7. Kuzmich, A. *et al.* Generation of nonclassical photon pairs for scalable quantum communication with atomic ensembles. *Nature* **423,** 731–734 (2003).
8. van der Wal, C. H. *et al.* Atomic memory for correlated photon states. *Science* **301,** 196–200 (2003).
9. Boyd, R. W. *Nonlinear Optics* (Academic, New York, 1992).
10. Boller, K. J., Imamoglu, A. & Harris, S. E. Observation of electromagnetically induced transparency. *Phys. Rev. Lett.* **66,** 2593–2596 (1991).
11. Hau, L. V. *et al.* Light speed reduction to 17 metres per second in an ultracold atomic gas. *Nature* **397,** 594–598 (1999).
12. Kash, M. M. *et al.* Ultraslow group velocity and enhanced nonlinear optical effects in a coherently driven hot atomic gas. *Phys. Rev. Lett.* **82,** 5229–5232 (1999).
13. Fleischhauer, M. & Lukin, M. D. Dark-state polaritons in electromagnetically induced transparency. *Phys. Rev. Lett.* **84,** 5094–5097 (2000).
14. Liu, C. *et al.* Observation of coherent optical information storage in an atomic medium using halted light pulses. *Nature* **409,** 490–493 (2001).
15. Phillips, D. F. *et al.* Storage of light in atomic vapor. *Phys. Rev. Lett.* **86,** 783–786 (2001).
16. Zibrov, A. S. *et al.* Transporting and time reversing light via atomic coherence. *Phys. Rev. Lett.* **88,** 103601 (2002).
17. Kocharovskaya, O., Rostovtsev, Y. & Scully, M. O. Stopping light via hot atoms. *Phys. Rev. Lett.* **86,** 628–631 (2001).
18. Andre, A. & Lukin, M. D. Manipulating light pulses via dynamically controlled photonic band gas. *Phys. Rev. Lett.* **89,** 143602 (2002).
19. Harris, S. E. Electromagnetically induced transparency with matched pulses. *Phys. Rev. Lett.* **70,** 552–555 (1993).
20. Cao, H. *et al.* Random laser action in semiconductor powder. *Phys. Rev. Lett.* **82,** 2278–2281 (1999).
21. Kogelnik, H. & Shank, C. V. Coupled wave theory of distributed feedback lasers. *J. Appl. Phys.* **43,** 2327–2335 (1972).
22. Yablonovich, E. *et al.* Donor and acceptor modes in photonic bandgap structures. *Phys. Rev. Lett.* **67,** 3380–3383 (1991).
23. Slusher, D. & Eggelton, B. (eds) *Nonlinear Photonic Crystals* (Springer, New York, 2003).
24. Harris, S. E., Field, J. E. & Imamoglu, A. Nonlinear optical processes using electromagnetically induced transparency. *Phys. Rev. Lett.* **64,** 1107–1110 (1990).
25. Schmidt, H. & Imamoglu, A. Giant Kerr nonlinearity obtained by electromagnetically induced transparency. *Opt Lett.* **21,** 1936–1938 (1996).
26. Hemmer, P. R. *et al.* Efficient low-intensity optical-phase conjugation based on coherent population trapping in sodium. *Opt. Lett.* **20,** 982–984 (1995).
27. Harris, S. E. & Hau, L. V. Nonlinear optics at low light levels. *Phys. Rev. Lett.* **82,** 4611–4614 (1999).
28. Lukin, M. D. & Imamoglu, A. Nonlinear optics and quantum entanglement of ultraslow single photons. *Phys. Rev. Lett.* **84,** 1419–1422 (2000).
29. Petrosyan, D. & Kurizki, G. Symmetric photon-photon coupling by atoms with Zeeman-split sublevels. *Phys. Rev. A* **65,** 033833 (2002).
30. Ottaviani, C., Vitali, D., Artoni, M., Cataliotti, F. & Tombesi, P. Polarization qubit phase gate in driven atomic media. *Phys. Rev. Lett.* **90,** 197902 (2003).

Acknowledgements We thank A. Andre, M. Eisaman, L. Childress, C. van der Wal, R. Walsworth, S. Zibrov and T. Zibrova for discussions, experimental help and comments on the manuscript. This work is supported by the NSF, the DARPA, the David and Lucille Packard Foundation and the Alfred Sloan Foundation. Partial support by the ONR (DURIP) is also acknowledged.

Competing interests statement The authors declare that they have no competing financial interests.

Correspondence and requests for materials should be addressed to M.D.L. (lukin@physics.harvard.edu).

An off-normal fibre-like texture in thin films on single-crystal substrates

C. Detavernier[1,2], A. S. Özcan[3], J. Jordan-Sweet[1], E. A. Stach[4], J. Tersoff[1], F. M. Ross[1] & C. Lavoie[1]

[1]*IBM T. J. Watson Research Center, Yorktown Heights, New York, New York 10598, USA*
[2]*Department of Solid State Physics, Ghent University, 9000 Ghent, Belgium*
[3]*Department of Physics, Boston University, Boston, Massachusetts 02215, USA*
[4]*National Center for Electron Microscopy, Lawrence Berkeley National Laboratory, Berkeley, California 94720, USA*

In the context of materials science, texture describes the statistical distribution of grain orientations. It is an important characteristic of the microstructure of polycrystalline films[1–5], determining various electrical, magnetic and mechanical properties. Three types of texture component are usually distinguished in thin films: random texture, when grains have no preferred orientation; fibre texture[6–10], for which one crystallographic axis of the film is parallel to the substrate normal, while there is a rotational degree of freedom around the fibre axis; and epitaxial alignment (or in-plane texture) on single-crystal substrates[11–15], where an in-plane alignment fixes all three axes of the grain with respect to the substrate. Here we report a fourth type of texture—which we call axiotaxy—identified from complex but